

K-factor Evaluation in a Hybrid Reverberation Chamber plus CATR OTA Testing Setup

Alejandro Antón Ruiz*, Samar Hosseinzadegan†, John Kvarnstrand†, Klas Arvidsson†, Andrés Alayón Glazunov*‡

*University of Twente, Enschede, The Netherlands, {a.antonruiz a.alayonglazunov}@utwente.nl

†Bluetest AB, Gothenburg, Sweden, name.familyname@bluetest.se

‡Linköping University, Norrköping Campus, Sweden, andres.alayon.glazunov@liu.se

Abstract—This paper investigates achieving diverse K-factors using a Reverberation Chamber (RC) with a Compact Antenna Test Range (CATR) system. It explores six hybrid "RC plus CATR" configurations involving different excitations of the Rich Isotropic Multipath (RIMP) field and CATR-generated plane waves, with some setups including absorbers. A fixed horn antenna points towards the CATR in all configurations. The study found that the null hypothesis of Rayleigh or Rician probability distributions for the received signal envelope could not be rejected, with RIMP setups primarily conforming to Rayleigh distribution and all setups showing Rician distribution. Various K-factors were obtained, but no generalizable method for achieving the desired K-factor was identified. The paper also estimates the K-factor as a function of frequency in the 24.25-29.5 GHz band. Smaller K-factors exhibit larger fluctuations, while larger K-factors remain relatively stable, with consistent fluctuations across the frequency range.

Index Terms—OTA, K-factor, Reverberation Chamber, CATR, mmWave.

I. INTRODUCTION

Over-The-Air (OTA) testing is key for developing and final product testing of wireless devices. It provides an assessment of real-life performance in controlled and repeatable conditions. OTA testing is currently the only option for fully integrated devices without any connectors available and for smart antenna systems [1]. It is impractical to characterize the device in infinite scenarios to ensure it always performs well. In practice, it is necessary to constrain the testing to a subset of meaningful scenarios. A relevant parameter for a testing scenario is the distribution of the received signal at the Device Under Test (DUT). Two limiting propagation scenarios can be identified: Rich Isotropic Multipath (RIMP) [2], and pure Line-Of-Sight (LOS), having an application in the Random Line-Of-Sight (Random-LOS) technique for OTA testing [3]. RIMP can be achieved in a Reverberation Chamber (RC), where a distribution of the received signal close to theoretical Rayleigh is generated if the chamber is properly designed [4]. Pure LOS can be achieved in an Anechoic Chamber (AC) or also in a semi-anechoic as used in the Electromagnetic Compatibility (EMC) tests.

The above two OTA environments offer excellent methods to recreate the ideal limiting propagation scenarios. However, real propagation environments are much more complex and may require combining the RIMP and the Compact Antenna

Test Range (CATR), depending on the application, as provided by the Bluetest solution. Thus, a LOS component and other Non-Line-Of-Sight (NLOS) components can be generated following a desired mixture. In this case, the distribution of the envelope of the received signal at the DUT should be a Rician. This distribution is characterized by two parameters: the K -factor defined as the ratio of the LOS over the NLOS powers, or the ratio between the unstirred power over the stirred power and the average received power [5]. An ideal RIMP scenario has a K -factor of 0 (or $-\infty$ dB), while pure LOS would have a K -factor of ∞ .

On another note, Millimeter Wave (mmWave) has been deemed as one of the enablers for Fifth Generation (5G) communications [6] due to the large available bandwidth at those frequencies. Due to the smaller wavelengths, diffraction is less relevant in the propagation. Also, channels at mmWave tend to be sparser, more directional, and have higher pathloss than sub-10 GHz frequencies. Therefore, it is expected that, in a general sense, K -factors of mmWave channels are higher than those of lower frequencies. Highly directive antennas such as phased arrays are used to overcome pathloss.

In this work, an investigation of the use of different configurations of a RC to achieve different K -factors is performed. The frequency range of interest is the lower FR2 bands for 5G (24.25 GHz to 29.5 GHz). The RC used for this experiment is a Bluetest RTS65, with the CATR option installed [7]. This allows to generate, in addition to the RIMP and the CATR environments separately, also other channels where both are mixed. In addition, using an absorber designed to attenuate the reflections coming from the CATR has also been considered in this work. The emulation of Rician channels in RCs is not new in the literature [8], [9], [10], [11]. However, to the author's best knowledge, this investigation has only been carried out at sub-6 GHz frequencies. This work considers using a CATR system at mmWave frequencies. Existing commercial products are used novelly since the Bluetest RTS65 was not originally designed to emulate Rician channels.

II. SIGNAL PROBABILITY DISTRIBUTION

A. Rayleigh Probability Distribution

In a RIMP environment, the distribution of the receive signal envelope by the DUT positioned in the test zone is Rayleigh and results from multipath interference. The scale parameter

σ fully determines the distribution [4]. In this case, the power follows an exponential distribution, with the parameter σ^2 as its only parameter, the average receive power. Estimating this parameter is straightforward by performing the mean of the obtained data.

B. Rician Probability Distribution

The Rician distribution model signals have two components: deterministic or direct LOS and NLOS random or scattered field components. The latter is Rayleigh distributed [8]. The K -factor is the power ratio of the LOS component over the NLOS component. In an ideal RC, which produced a perfect Rayleigh distribution, the K -factor would be 0 (or $-\infty$ dB). However, that is not achievable in practice. In the RC context, the K -factor can be better understood as

$$K = P_d/P_s, \quad (1)$$

where P_s is the stirred power, and P_d is the power of the unstirred paths, which includes a direct LOS when the CATR is used.

In this work, we have decided to use the estimator found in [9] since it is unbiased. A major note is that this estimator requires acquiring the complex value of the transmission parameter S_{21} . While we do not reproduce the estimator equation, we say that it depends on the number of samples, which are assumed to be independent. This we take for granted in this work. However, future work will fully consider their independence and impact on the estimation.

III. EXPERIMENTAL SETUP

A. Chamber

Fig. 1 shows the experimental setup using a Bluetest RTS65 RC chamber with the CATR option installed [7]. The chamber is designed to be used as a 2-in-1 test system, providing a RIMP field in the test zone when it is excited through the RIMP port or a LOS only when it is excited through the CATR port. The latter mode uses absorbers on the walls, enabling radiation pattern measurements within the same space.

The CATR mode of the chamber is realized by the use of a parabolic reflector with a dual-polarized antenna feed shown in yellow in Fig. 1. The generated plane wave has a 0.6 dB amplitude and a 4° phase ripples. The Standard Deviation (STD) ripples are at frequencies from 24.25 – 42 GHz within a 30 cm diameter cylindrical test zone [12] (see Fig. 2). The polarization of the antenna is selected through a passive switch. To handle the reflections coming from the reflector or the DUT, a set of carbon-loaded foam absorbers is placed around the chamber, as shown in Fig. 2. Except for the absorber on the wall towards which the plane wave is directed ("back absorber"), all the other absorbers are Frequency Selective Absorber (FSA). They are covered by a metallic honeycomb pattern designed with spacing such that the sub-6 GHz frequency signals for which the chamber is also designed to operate in RIMP mode are not significantly attenuated by the FSA. However, they provide significant attenuation at mmWave. The back absorber has the same material and

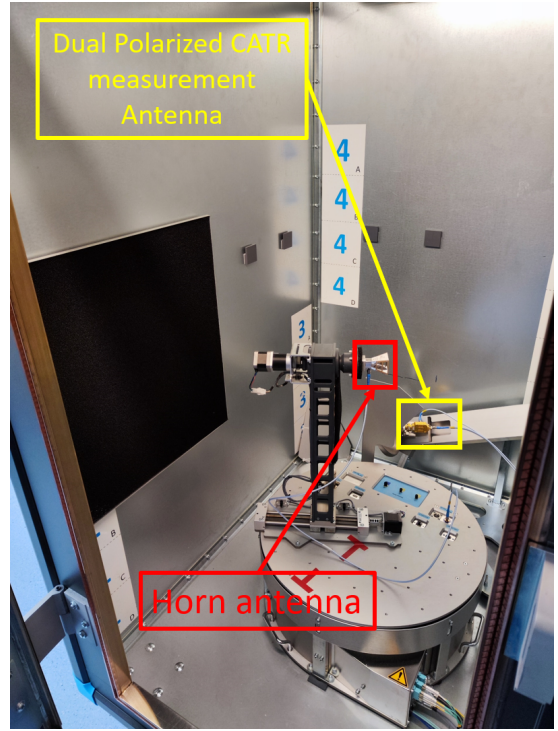


Fig. 1. Bluetest RTS65 with the CATR option and the back absorber installed. The dimensions of the chamber are 1945x2000x1440 mm (WxHxD).

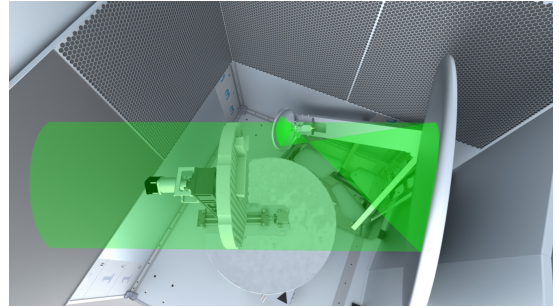


Fig. 2. CAD render showing geometry and signal flow (in green). The test zone is located within the lightest green volume. Source: [7].

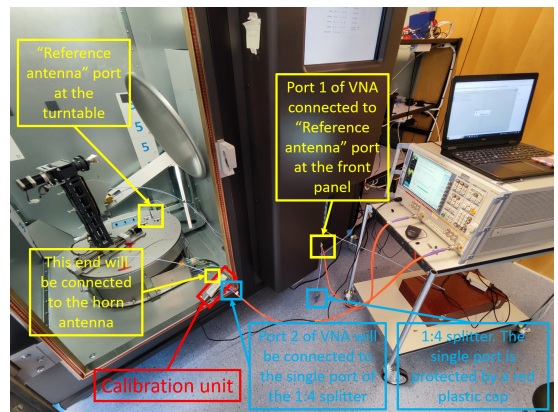


Fig. 3. Experiment setup for calibrating the VNA.

size as the FSA, except that the metallic honeycomb part is removed, thus providing better absorption. This is because most of the energy coming from the reflector is directed to this back absorber. In this work, only the back absorber scenario was considered (see Fig. 1).

B. Antenna

The experiment uses a linearly-polarized double ridged Horn Antenna (HA), designed to operate from 4.5 – 50 GHz [13]. The choice of antenna is because of its directional pattern and an accessible port so that the complex-valued S_{21} can be measured to estimate the K -factor. The use of a directive antenna for mmWave experiments is highly relevant because the obtained K -factor can serve as a reference value for other directive antennas. Even though results are valid for this specific antenna because of the spatial filtering that the directive antenna performs, they might be similar to those obtained for a different antenna with similar directivity. For example, results obtained with a phased array can be compared to the reference value. However, a characterization of the K -factor using an omnidirectional antenna is acknowledged to be relevant but is left for future work.

C. Considered test cases

A total of six cases are considered:

- NoAs_R: no absorbers, only RIMP excitation.
- NoAs_C_PS1: no absorbers, only CATR excitation with the matching polarization of the HA.
- NoAs_RC_PS1: no absorbers, RIMP and CATR excitation with the CATR in the matching polarization of the HA.
- BAs_R: back absorber, only RIMP excitation.
- BAs_C_PS1: back absorber, only CATR excitation with the matching polarization of the HA.
- BAs_RC_PS1: back absorber, RIMP and CATR excitation with the CATR in the matching polarization of the HA.

Note that PS1 stands for "Passive Switch set to 1", which means that the CATR port is routed to the port of the reflector feeder antenna designed as "1", which is the one that produces the polarization that matches that of the HA, as it was installed in the experiment.

D. Instrument and measurement

1) *Cabling*: To perform this experiment, a 1:4 splitter was used to connect one of the VNA ports to the RIMP and/or CATR ports, while the other port of the VNA was connected to the HA via a port in the front panel of the chamber. For RIMP or CATR only measurements, only one of the four splitter ports was used, while the other three were terminated. Two of the four ports were used in the RIMP plus CATR measurements, while the other two were terminated.

2) *VNA and measurement configuration*: The VNA was configured to perform a S_{21} sweep in the frequency from 24 – 29.5 GHz with a 10 MHz step, although only the 24.25 to 29.5 GHz range is presented here to adequate to the FR2 bands. An Intermediate Frequency (IF) bandwidth of 1 KHz was used.

For each frequency point, a total of 600 samples were collected. Those 600 samples were taken at 600 unique positions of the two mode-stirrers of the chamber located on the ceiling and right wall while keeping the turntable fixed where the HA was pointed at the reflector. It is worth noting in Fig. 1 that the "right wall" is located on the right, behind the large reflector and the metallic plate behind it. Hence, keeping the antenna in a fixed position relative to the reflector was done to have a more controlled interaction between the HA and the reflector. However, it is left for future work to use the turntable as a stirring mechanism, making the results less dependent on the direction towards which the main beam of the antenna is pointing.

Regarding the VNA calibration, the calibration plane was, on one side, at the port of the HA and, on the other side, at the single port of the 1:4 splitter. This is depicted in more detail in Fig 3.

IV. RESULTS

Fig. 4 shows the results of both K -factor (left y-axis) and $|S_{21}|^2$ (right y-axis) as a function of the considered frequency. The estimated K -factor is computed for each frequency point of the considered band and shown as "No SW," where SW stands for Sliding Window. Then, an averaging of the K -factor over SWs of 100, 200, and 400 MHz is presented. This averaging is common in the literature to reduce statistical variations and is known as frequency stirring [5] and, in this case, it can approximate what the average K -factor value of a 5G FR2 channel of 100, 200, or 400 MHz centered at the x-axis frequency would be in this setup. The $|S_{21}|^2$ is plotted to assess what occurs in each studied case regarding the system losses. On the other hand, Table. I shows some relevant statistics of both the K -factor and $|S_{21}|^2$, for the whole frequency range, including the results of the one-sample Kolmogorov-Smirnov tests that were performed to assess if the distributions of the 600 samples at each frequency could come from Rayleigh or Rician distributions. The presented result in Table I is the pass rate of these Goodness of Fit (GoF) tests, which indicates the percentage of frequencies for which it could not be rejected that the samples $|S_{21}|$ came from a fitted Rayleigh or Rician distribution, at a 5% significance level. Regarding this, the results align with the expectations since for the RIMP only excitations, the pass rate for Rayleigh is high, while, for the cases with CATR excitation, it is 0. The pass rate for Rician distribution is high in all cases, aligned with the expectations, which enables the use of the K -factor as a relevant parameter for all cases. Note that the Rayleigh distribution is a particular case of the Rician distribution. For the CATR only, even if we had a pure LOS contribution, we

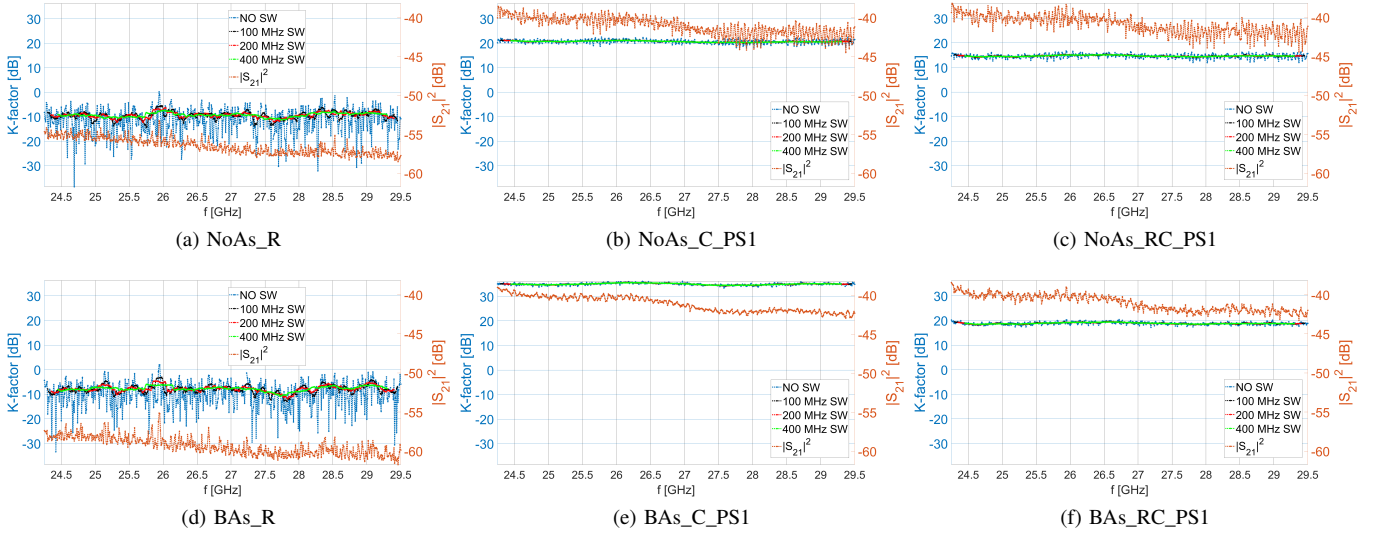


Fig. 4. K -factor for different Sliding Windows (SWs) and $|S_{21}|^2$, as a function of the frequency; where only $|S_{21}|^2$ belongs to the right y-axis.

TABLE I
RELEVANT STATISTICS OF K -FACTOR AND $|S_{21}|^2$.

Case	Avg. $ S_{21} ^2$ [dB]	Avg. K -factor [dB]	Normalized STD K -factor	Dynamic range K -factor [dB]	GoF pass rate Rayleigh	GoF pass rate Rician
NoAs_R	-56.37	-9.28	1.00	38.71	98.29%	99.43%
NoAs_C_PS1	-40.92	20.70	0.17	4.55	0.00%	100.00%
NoAs_RC_PS1	-40.79	14.70	0.18	4.72	0.00%	100.00%
BAs_R	-59.19	-7.66	1.05	35.31	97.91%	100.00%
BAs_C_PS1	-41.01	35.01	0.10	2.78	0.00%	100.00%
BAs_RC_PS1	-40.94	18.82	0.13	3.22	0.00%	100.00%

would still have a particular case of Rician distribution (with ∞ K -factor).

In Fig. 4, it can be observed that the K -factor heavily fluctuates, in relative terms, i.e., in dB, whenever the chamber is not excited through the CATR port (a, d), remaining much more stable when the CATR port is excited (b, c, e, f). This can also be observed in Table I, in both the dynamic range (or peak-to-peak variation) and the normalized STD of the K -factor. The stability when the CATR is excited is caused by the fact that the LOS component, which is relatively stable with frequency, dominates over the stirred components. The large variations of K -factor when RIMP is only excited are caused by several factors. On the one hand, there is the effect of limited sampling in conjunction with a low K -factor, as observed in Fig. 8 of [9]. In short, the Confidence Intervals (CIs) (in dB scale) for the estimates of the K -factor, which can be found in (43) and (44) from [9], when K -factor is low, are broadened significantly (in dB scale). For reference, the 95% CI for 600 samples and a K -factor of -9.28 dB is $[-11.09, -8.01]$ dB, while, for a K -factor of 35.01 dB, it is $[34.65, 35.35]$ dB. However, the K -factor varies much further than those confidence intervals, so it is likely that the actual K -factor experiences large frequency variations when it is low. On the other hand, these variations could also be partially due to the absence of turntable stirring. This leaves the antenna

in a fixed position, resulting in frequency-dependant unstirred paths at the antenna position. Therefore, it would be interesting to use turntable stirring and observe if variations are smoothed.

When the back absorber is placed, there is an increase in the system's losses, i.e., average $|S_{21}|^2$. In particular, the total averaged $|S_{21}|^2$ decreases in 2.82 dB for the RIMP excitation only, 0.09 dB for the CATR excitation only, and 0.15 dB for the RIMP and CATR excitation. As expected, the increase in the system's losses in relative terms, i.e., in dB, is lower for the cases where the CATR is on and, therefore, the dominant contribution is that of the LOS, which does not interact with the absorber. It can be observed that there is a direct relation between higher average K -factor and smaller increases in the system's losses, being the CATR only case the one with the smallest increase, of just 0.09 dB.

As for the use of SWs, they only make a difference in the RIMP only cases since there is not such a large variation on the K -factor with the frequency for the rest of the considered cases. For the RIMP only cases, the 100 MHz SW already provides a relevant smoothing, which improves with the larger SWs. However, even with the 400 MHz SW, there are some variations of the K -factor with the frequency. This is not observed when the CATR is excited. This result is relevant because it implies that within the presented cases, the proposed setup can only provide a quite frequency-stable K -factor

when the CATR is excited, resulting in high K -factors. Conversely, for low K -factors, it cannot provide, in relative terms, a frequency-stable K -factor, which occurs when only the RIMP branch is excited. As a point for future work, it is left to assess if a frequency-stable, low (at least lower than the ones obtained when the CATR is excited) K -factor can be achieved by, e.g., exciting the CATR and RIMP, but attenuating the CATR branch, or using turntable stirring. On another note, it is also worth noting that the K -factor variations do not follow any clear trend with respect to the frequency, i.e., there is not an appreciable linear dependency of neither the SW averaged K -factor nor the K -factor variation.

Finally, when observing the full frequency band averaged K -factor from Table I, it is worth noting that the fact of adding the back absorber increases the K -factor in around 14.31 dB when only the CATR is excited, but only in around 4.12 dB when both the RIMP and CATR are excited. Therefore, the estimated stirred power decreases in 14.36 dB for the CATR and 4.18 dB for the RIMP and CATR case, when adding the back absorber. As for the estimated unstirred power, it decreases in 0.06 dB for both the CATR only and the RIMP and CATR cases, when adding the back absorber. Therefore, it is clear that the addition of the back absorber has a greater effect on reducing the stirred power coming from the CATR by capturing a significant amount of the energy that is not directly coupled to the horn antenna. This leads to a greater increase of K -factor for the CATR only case than for the RIMP and CATR one. As for the RIMP only case, adding the back absorber decreases the K -factor of 1.62 dB. This comes from a decrease of the estimated stirred power of 3.03 dB and a decrease of the estimated unstirred power of 1.41 dB. All in all, adding the back absorber for RIMP excitation only decreases the resemblance of the environment to a pure RIMP one.

V. CONCLUSION

This paper presents six RC setups equipped with a CATR system operating at the 24.25 – 29.5 GHz band, analyzing field distribution using one-sample Kolmogorov-Smirnov GoF tests and focusing on K -factor. The GoF tests align with expectations, confirming a Rician distribution for all cases and a Rayleigh distribution for RIMP-only excitation. Different K -factors are achievable with varying setups. Low estimated K -factors are less stable with frequency relative to high K -factors. K -factor variations and sliding window averages show no frequency dependence. The directional horn antenna used in this study aims to provide a reference for directive antennas in spatially selective channels. However, further work can improve predictability by incorporating turntable stirring and omnidirectional antennas. This will also allow us to characterize the K -factor independently from the orientation

of the antenna, at least on the 2D horizontal plane. Other setups should be explored, such as attenuators in RIMP and/or CATR configurations. This work marks an initial step toward utilizing a commercialized mmWave product for novel OTA testing with a controllable K -factor.

ACKNOWLEDGMENT

The work of Alejandro Antón is supported by the European Union's Horizon 2020 Marie Skłodowska-Curie grant agreement No. 955629. Andrés Alayón Glazunov also kindly acknowledges funding from the ELLIIT strategic research environment (<https://elliit.se/>).

REFERENCES

- [1] P. Zhang, X. Yang, J. Chen, and Y. Huang, "A survey of testing for 5G: Solutions, opportunities, and challenges," *China Communications*, vol. 16, no. 1, pp. 69–85, 2019.
- [2] Kildal, Per-Simon and Carlsson, Jan, "New approach to OTA testing: RIMP and pure-LOS reference environments & a hypothesis," in *2013 7th European Conference on Antennas and Propagation (EuCAP)*, 2013, pp. 315–318.
- [3] P.-S. Kildal, A. A. Glazunov, J. Carlsson, and A. Majidzadeh, "Cost-effective measurement setups for testing wireless communication to vehicles in reverberation chambers and anechoic chambers," in *2014 IEEE Conference on Antenna Measurements & Applications (CAMA)*, 2014, pp. 1–4.
- [4] M. Andersson, A. Wolfgang, C. Orlenius, and J. Carlsson, "Measuring performance of 3GPP LTE terminals and small base stations in reverberation chambers," in *Long Term Evolution*. Auerbach Publications, 2016, pp. 427–472.
- [5] X. Chen, P.-S. Kildal, and S.-H. Lai, "Estimation of Average Rician K-Factor and Average Mode Bandwidth in Loaded Reverberation Chamber," *IEEE Antennas and Wireless Propagation Letters*, vol. 10, pp. 1437–1440, 2011.
- [6] T. S. Rappaport, S. Sun, R. Mayzus, H. Zhao, Y. Azar, K. Wang, G. N. Wong, J. K. Schulz, M. Samimi, and F. Gutierrez, "Millimeter Wave Mobile Communications for 5G Cellular: It Will Work!" *IEEE Access*, vol. 1, pp. 335–349, 2013.
- [7] J. Kvarnstrand, P. Svedjenäs, E. Silfverswärd, and H. Helmius, "Integrating LoS and RIMP Measurements in a Single Test Environment," in *2021 15th European Conference on Antennas and Propagation (EuCAP)*, 2021, pp. 1–5.
- [8] C. L. Holloway, D. A. Hill, J. M. Ladbury, P. F. Wilson, G. Koepke, and J. Coder, "On the Use of Reverberation Chambers to Simulate a Rician Radio Environment for the Testing of Wireless Devices," *IEEE Transactions on Antennas and Propagation*, vol. 54, no. 11, pp. 3167–3177, 2006.
- [9] C. Lemoine, E. Amador, and P. Besnier, "On the K -Factor Estimation for Rician Channel Simulated in Reverberation Chamber," *IEEE Transactions on Antennas and Propagation*, vol. 59, no. 3, pp. 1003–1012, 2011.
- [10] A. A. Glazunov, S. Prasad, and P. Handel, "Experimental Characterization of the Propagation Channel Along a Very Large Virtual Array in a Reverberation Chamber," in *Progress In Electromagnetics Research B*, vol. 59, 2014, pp. 205–217.
- [11] J. D. Sanchez-Heredia, J. F. Valenzuela-Valdes, A. M. Martinez-Gonzalez, and D. A. Sanchez-Hernandez, "Emulation of MIMO Rician-Fading Environments With Mode-Stirred Reverberation Chambers," *IEEE Transactions on Antennas and Propagation*, vol. 59, no. 2, pp. 654–660, 2011.
- [12] Bluetest. (2020) 5G OTA DEVICE TESTING IN THE RTS65. [Online]. Available: https://www.bluetest.se/files/5G_RevA.pdf
- [13] RF SPIN. (2022) DRH50 Datasheet. [Online]. Available: <https://www.rfspin.com/wp-content/uploads/2022/04/DRH50-ÅŞ-RF-SPIN.pdf>